

Lepton reconstruction in the ENUBET tagger

F. Pupilli,^{c,*} F. Acerbi,^{a,b} I. Angelis,^x M. Bonesini,^{e,f} F. Bramati,^f A. Branca,^{e,f}
 C. Brizzolari,^{e,f} G. Brunetti,^f M. Calviani,^r S. Capelli,^{e,p} S. Carturan,^{d,g}
 M.G. Catanesi,^h S. Cecchini,ⁱ N. Charitonidis,^r F. Cindolo,ⁱ G. Collazuol,^{c,d} F. Dal
 Corso,^c C. Delogu,^{c,d} G. De Rosa,^{j,k} A. Falcone,^{e,f} A. Gola,^a B. Goddard,^r F. Iacob,^{c,d}
 C. Jollet,^l V. Kain,^r B. Kliček,^m Y. Kudenko,^{n,u,v} Ch. Lampoudis,^x M. Laveder,^{c,d}
 A. Longhin,^{c,d} L. Ludovici,^o E. Lutsenko,^{e,p} L. Magaletti,^{h,q} G. Mandrioli,ⁱ
 A. Margotti,ⁱ V. Mascagna,^{e,p} N. Mauri,ⁱ L. Meazza,^{e,f} A. Meregaglia,^l M. Mezzetto,^c
 M. Nessi,^r A. Paoloni,^t M. Pari,^{c,d,r} E.G. Parozzi,^{e,f,r} L. Pasqualini,^{i,s} G. Paternoster,^a
 L. Patrizii,ⁱ M. Pozzato,ⁱ M. Prest,^{e,p} E. Radicioni,^h C. Riccio,^{j,k} A.C. Ruggeri,^{j,k} D.
 Sampsonidis,^x C. Scian,^{c,d} G. Sirri,ⁱ M. Stipčević,^m M. Tenti,ⁱ F. Terranova,^{e,f}
 M. Torti,^{e,f,1} S. E. Tzamarias,^x E. Vallazza,^e F.M. Velotti^r and L. Votano^t

^aFondazione Bruno Kessler (FBK), Via Sommarive 18 - 38123 Povo (TN), IT

^bINFN-TIFPA, Università di Trento, Via Sommarive 14 - 38123 Povo (TN), IT

^cINFN Sezione di Padova, via Marzolo 8 - 35131 Padova, IT

^dUniversità di Padova, via Marzolo 8 - 35131 Padova, IT

^eINFN Sezione di Milano-Bicocca, Piazza della Scienza 3 - 20133 Milano, IT

^fUniversità di Milano-Bicocca, Piazza della Scienza 3 - 20133 Milano, IT

^gINFN, Laboratori Nazionali di Legnaro, Viale dell'Università 2 - 35020 Legnaro (PD), IT

^hINFN Sezione di Bari, Via Giovanni Amendola 173 - 70126 Bari, IT

ⁱINFN Sezione di Bologna, viale Berti-Pichat 6/2 - 40127 Bologna, IT

^jINFN, Sezione di Napoli, Strada Comunale Cinthia - 80126 Napoli, IT

^kUniversità "Federico II" di Napoli, Corso Umberto I 40 - 80138 Napoli, IT

^lCENBG, Université de Bordeaux, CNRS/IN2P3, 33175 Gradignan, FR

^mCenter of Excellence for Advanced Materials and Sensing Devices, Ruder Boskovic Institute, HR-10000 Zagreb, HR

ⁿInstitute for Nuclear Research of the Russian Academy of Sciences, 117312 Moscow, RU

^oINFN Sezione di Roma 1, Piazzale A. Moro 2, 00185 Rome, IT

^pUniversità degli Studi dell'Insubria, Via Valleggio 11 - 22100 Como, IT

^qUniversità degli Studi di Bari, Via Giovanni Amendola 173 - 70126 Bari, IT

^rCERN, Esplanade des particules - 1211 Genève 23, CH

^sUniversità degli Studi di Bologna, viale Berti-Pichat 6/2 - 40127 Bologna, IT

^tINFN, Laboratori Nazionali di Frascati, via Fermi 40 - 00044 Frascati (Rome), IT

^uNational Research Nuclear University "MEPhI", 115409 Moscow, RU

^vMoscow Institute of Physics and Technology, 141701 Moscow region, RU

^xAristotle University of Thessaloniki. Thessaloniki 541 24, GR

E-mail: fabio.pupilli@pd.infn.it

*Speaker

The ENUBET project aims at demonstrating the feasibility of a monitored neutrino beam in which the measurement of associated charged leptons in the instrumented decay region of a conventional beam is used to constrain the neutrino flux to unprecedented precision ($O(1\%)$). Large angle muons and positrons from kaon decays are detected on the decay tunnel walls equipped with a sampling calorimeter with longitudinal, radial and azimuthal segmentation. After a brief description of the ENUBET beamline and of the detectors employed in the lepton tagger, the analysis chain for the event reconstruction, the background suppression and the identification of positrons and muons will be described.

*** *The 22nd International Workshop on Neutrinos from Accelerators (NuFact2021)* ***
*** *6–11 Sep 2021* ***
*** *Cagliari, Italy* ***

1. The ENUBET beamline and the lepton tagger

The goal of ENUBET is to design a facility in which the uncertainty on the ν_e and the ν_μ flux is kept below 1%, thus removing the main systematics for a high precision neutrino cross section measurement at the GeV scale, that would be of paramount importance for next generation long baseline oscillation experiments. The flux is monitored by measuring the charged leptons produced in association with the neutrinos in the instrumented decay region of the facility [1]. The rate of large angle positrons and muons on the decay tunnel walls is used as a proxy to determine the neutrino flux from K_{e3} ($K^+ \rightarrow \pi^0 e^+ \nu_e$) and $K_{\mu\nu}$ ($K^+ \rightarrow \mu^+ \nu_\mu$, $K^+ \rightarrow \pi^0 \mu^+ \nu_\mu$) decays respectively, while low angle muons from pions can be measured by muon monitor stations after the hadron dump, thus providing a full constraint on the overall flux [2, 3]. The ENUBET beamline is designed to provide a narrow-band neutrino beam by focusing towards the 40 m long decay tunnel positively charged mesons with a momentum bite of 5-10% centered at 8.5 GeV/c. The shielding elements are carefully fine tuned to suppress the beam halo on the tunnel instrumentation that could spoil the lepton identification capabilities, and to retain at the same time a large enough meson yield [4].

The lepton tagger (Fig. 1) is based on a sampling calorimeter as a cost-effective solution to perform $e/\pi/\mu$ separation, placed on the whole surface of the 1 m radius, 40 m long decay tunnel. The calorimeter is segmented in the longitudinal, radial and azimuthal coordinates and its basic unit, called LCM (Lateral Compact Module), has a 3×3 cm² transverse size and is composed by a stack of five 0.7 cm thick scintillator tiles interleaved with five 1.5 cm thick iron tiles. Three radial layers of LCM are foreseen. The instrumentation is complemented by rings of plastic scintillator doublet tiles (3×3 cm², 0.7 cm thick) below the calorimeter (t0-layer), acting as a photon veto to suppress the π^0 background and providing timing information. Both the detectors are read out by WLS fibers placed on the frontal faces of the tiles and coupled to SiPMs [5, 6].

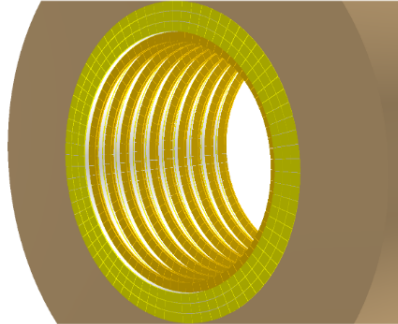


Figure 1: Schematics of a part of the ENUBET lepton tagger. The three layers of LCM composing the calorimeter are shown in light green. The rings of scintillator tiles composing the t0-layer below the calorimeter are shown in yellow. WLS fibers (not shown) bring the light above a borated polyethylene shielding (light brown) where the SiPMs are located.

2. The ENUBET tagger simulation

The full instrumentation of the ENUBET tagger has been implemented in detail in a GEANT4 package (G4TAG). The simulation includes the propagation and decay up to the hadron dump of

particles provided at the tunnel entrance by a standalone GEANT4 simulation of the transfer line. The response of the detectors in the tunnel is simulated at hit level, not considering the scintillation process and light propagation. An hit rate of $O(1 \text{ MHz})$ is expected on each detector channel. In order to assess the effects of pile-up on the overall detector performance a software framework has been implemented to simulate the tagger response at single channel level. Each visible energy deposits coming from the G4TAG simulation is converted into photons hitting the SiPM with a conversion factor (15 p.e./MeV) derived from previous test beam data on tagger prototypes [6]. The SiPM response is then simulated using the GosSIP software tool [7] and the generated waveforms are processed by a pulse detection algorithm providing the time and the amplitude (converted back in MeV) of the found peaks.

3. Positron identification

The first step for the charged lepton reconstruction in the tagger is the event building: energy deposits correlated in space and time within predefined cuts are clustered starting from an event seed in the innermost calorimeter layer. In order to preselect positron candidates and to suppress mip-like events, a visible energy greater than 28 MeV is required for the seed: indeed the Landau fit of the energy released by a mip in a LCM has a most probable value of $\sim 6.5 \text{ MeV}$.

A multi-layer perceptron neural network (MLPNN) with 19 input variables is then employed to identify an high purity sample of K_{e3} positrons. It exploits: 1) the energy deposition pattern in the calorimeter to separate the more localized positron events from the hadronic showers induced by pions and from the muon single track topologies; 2) the energy deposition in the t0-layer to suppress the residual photon background; 3) the position of the event to reduce the beam halo background that is mostly concentrated in the first part of the tagger. By choosing a cut on the neural network classifier that maximizes the product of the efficiency and the purity in the selection, a signal-to-noise ratio of ~ 2 is achieved with a positron identification efficiency of 22%, that includes also the geometrical acceptance of the tagger ($\sim 50\%$).

Fig. 2 shows the distribution along the tunnel of the events reconstructed by the event builder (left) and after the neural network discrimination (right). The dominant background is represented by beam induced positrons.

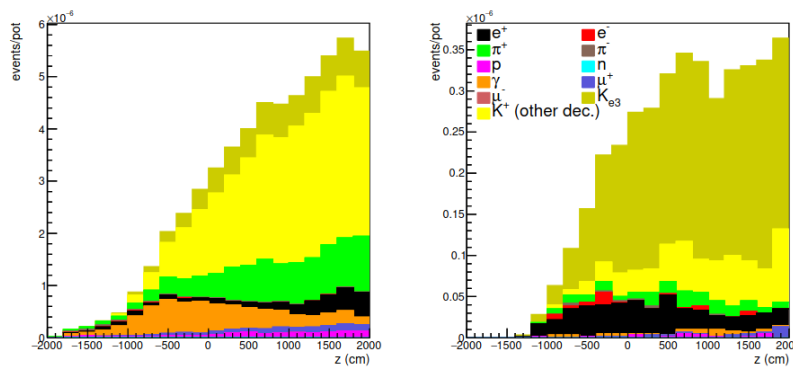


Figure 2: Longitudinal position of selected events at different stages in the selection of K_{e3} positron events: (left) after the event building; (right) after the NN discrimination.

4. Muon identification

As for the positrons, the reconstruction of muons from kaon decays begins with the event building. However, in this case it is triggered by a seed compatible with the energy deposition of a mip ($5 < E < 15$ MeV) and the clustering is oriented towards the search of aligned hits in order to enhance the preselection of muon candidates.

The signal-background discrimination is achieved with a MLPNN with 13 input variables that takes into account the energy deposition pattern together with the impact point along the tunnel: indeed the latter is particularly effective in suppressing the background from halo muons, that is more abundant in the first half of the tunnel, as can be seen from Fig. 3.

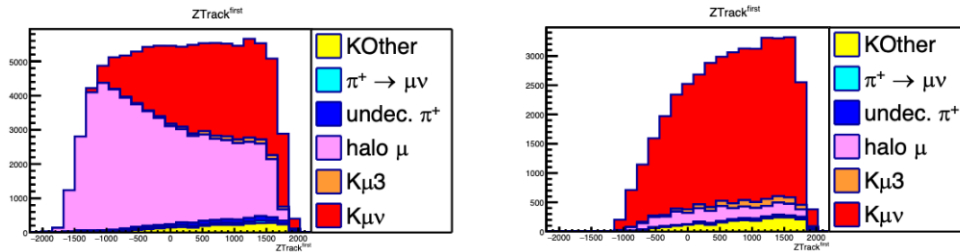


Figure 3: Longitudinal position of selected events at different stages in the selection of $K_{\mu\nu}$ muon events: (left) after the event building; (right) after the NN discrimination.

The muon identification efficiency obtained cutting at the neural network classifier value that maximizes the efficiency times purity is 34%, with a signal-to-noise ratio of ~ 6 . The larger purity with respect to the positron case is mostly driven by the more favorable branching ratio of $K_{\mu\nu}$ with respect to the K_{e3} one.

Acknowledgments

This project has received funding from the European Union’s Horizon 2020 Research and Innovation programme under Grant Agreement no. 681647 and by the Italian Ministry of Education and Research – MIUR (Bando “FARE”, progetto NuTech).

References

- [1] A. Longhin, L. Ludovici and F. Terranova, *Eur. Phys. J. C* **75** (2015) 155.
- [2] F. Acerbi *et al.* CERN-SPSC-2021-013, SPSC-SR-290, Geneva, 2021.
- [3] G. Brunetti *et al.*, *The ENUBET project: a monitored neutrino beam*, these proceedings.
- [4] M. Pari *et al.*, *Development and optimization of the ENUBET beamline*, these proceedings.
- [5] F. Iacob *et al.*, *Detector R&D for the ENUBET instrumented decay region*, these proceedings.
- [6] F. Acerbi *et al.*, *JINST* **15** (2020) 08, P08001.
- [7] P. Eckert *et al.*, *JINST* **7** (2012) P08011.